

AperTO - Archivio Istituzionale Open Access dell'Università di Torino

Solid lipid nanoparticles by coacervation loaded with a methotrexate prodrug: preliminary study for glioma treatment

This is the author's manuscript

Original Citation:

Availability:

This version is available <http://hdl.handle.net/2318/1627489> since 2017-05-20T22:06:09Z

Published version:

DOI:10.2217/nnm-2016-0380

Terms of use:

Open Access

Anyone can freely access the full text of works made available as "Open Access". Works made available under a Creative Commons license can be used according to the terms and conditions of said license. Use of all other works requires consent of the right holder (author or publisher) if not exempted from copyright protection by the applicable law.

(Article begins on next page)

This is the author's final version of the contribution published as:

Battaglia, L; Muntoni, E; Chirio, D; Peira, E; Annovazzi, L; Schiffer, D; Mellai, M; Riganti, C; Salaroglio, Ic; Lanotte, M; Panciani, P; Capucchio, Mt; Valazza, A; Biasibetti, E; Gallarate, M. Solid lipid nanoparticles by coacervation loaded with a methotrexate prodrug: preliminary study for glioma treatment. NANOMEDICINE. 12 pp: 639-656.
DOI: 10.2217/nmm-2016-0380

The publisher's version is available at:

<http://www.futuremedicine.com/doi/pdf/10.2217/nmm-2016-0380>

When citing, please refer to the published version.

Link to this full text:

<http://hdl.handle.net/2318/1627489>

Solid lipid nanoparticles by coacervation loaded with a methotrexate prodrug: preliminary study for glioma treatment

Authors:

Luigi Battaglia^{1*}, Elisabetta Muntoni¹, Daniela Chirio¹, Elena Peira¹, Laura Annovazzi², Davide Schiffer², Marta Mellai², Chiara Riganti³, Iris Chiara Salaroglio³, Michele Lanotte⁴, Pierpaolo Panciani⁴, Maria Teresa Capucchio⁵, Alberto Valazza⁵, Elena Biasibetti⁵, Marina Gallarate¹.

1 – Università degli Studi di Torino - Dipartimento di Scienza e Tecnologia del Farmaco, Torino

2 – Centro Ricerche di Neurobiooncologia, Policlinico di Monza Foundation, Vercelli, Italy

3 - Università degli Studi di Torino - Dipartimento di Oncologia, Orbassano

4 - Università degli Studi di Torino - Dipartimento di Neuroscienze, Torino

5 - Università degli Studi di Torino - Dipartimento di Scienze Veterinarie, Grugliasco

*Corresponding Author:

via Pietro Giuria 9, Torino

phone: +390116707668

email: luigi.battaglia@unito.it

Abstract

Aims

Methotrexate loaded biocompatible nanoparticles were tested for preliminary efficacy in glioma treatment.

Materials and methods

Behenic acid nanoparticles, prepared by coacervation method, were loaded with the ester prodrug didodecylmethotrexate, which was previously tested *in vitro* against glioblastoma human primary cultures. Nanoparticles conjugation with an ApoE mimicking chimera peptide was performed to obtain active targeting to the brain.

Results and Conclusions

Biodistribution studies in healthy rats assessed the superiority of ApoE conjugated formulation, which was tested on a F98/Fischer glioma model. Differences were observed in tumor growth rate (measured by MRI) between control and treated rats. *In vitro* tests on F98 cultured cells assessed their susceptibility to treatment, with consequent apoptosis, and allowed us to explain the apoptosis observed in glioma models.

Keywords: solid lipid nanoparticles, coacervation, methotrexate, glioma, chimera peptide, apolipoprotein E, biodistribution, apoptosis, magnetic resonance imaging, orthotopic model

1. Introduction

Glioblastoma multiforme (GBM), a grade IV glioma, is the most frequently occurring and invasive primary tumor of the central nervous system, which causes about 4% of cancer-associated-deaths, making it one of the inescapably fatal cancers. With present therapies, using state-of-the-art technologies, the median survival is about 14 months, and 2-year survival rate is merely 3–5%. Currently, GBM pharmacological therapy is only adjuvant: innovative pharmacological treatment is needed, but most of the drugs do not cross the blood–brain barrier (BBB), which is one of the major obstacles to GBM treatment.

Nanocarriers are drug transport systems that have gained huge research focus over the last few decades for site-specific drug delivery, including brain delivery [1].

In particular, solid lipid nanoparticles (SLN) have been proposed as innovative chemotherapeutic agent vehicles for experimental GBM treatment, owing to their ability to enhance drug uptake by cells and to evade P-glycoprotein (Pgp) efflux system. It is well known that SLN are subjected to endocytosis from endothelial cells, and can also be exploited as for passive and, if opportunely surface-modified, for active targeting [2].

An innovative solvent-free SLN production technique was developed by our research group [3], based on fatty acid precipitation that occurs when pH of a fatty acid alkaline salt micellar solution is lowered by acidification, in the presence of an appropriate polymeric stabilizer; this process was defined as “coacervation”.

In previous experimental works, performed by our research group, SLN prepared according to the coacervation technique were exploited as anticancer delivery systems [4, 5, 6, 7], also for GBM treatment [6, 7]. Methotrexate (MTX) is difficult to entrap within SLN due to its hydrophilicity. Didoceylmethotrexate (ddMTX), a lipophilic MTX ester, instead, can be easily, loaded ddMTX

was synthesized and loaded in SLN, prepared through the coacervation technique. ddMTX loaded SLN were tested on GBM neurospheres derived from human primary tumors: the cytotoxicity of the parental drug was maintained, meaning that the chemical lipophilization reaction did not alter its biological activity. The maintenance of biological activity can partly be due to the cleavable nature of the ester bond, which is mainly present in ddMTX. Moreover, ddMTX-loaded SLN were tested on an artificial BBB model with promising results [8]. Moreover, although the reduced particle size (below 200 nm) is generally thought to be required in order to obtain long circulating nanoparticles and, consequently, BBB overcoming, interesting findings were obtained from a recent study, employing purpose-built fluorescent polybutylcyanoacrylate (PBCA) nanoparticles. An imaging study in animals, performed by *in vivo* confocal neuroimaging (ICON), revealed that also particles larger than 400 nm can cross the BBB: it is the particle surface, instead, that determines the crossing, with non-ionic surfactants enhancing brain uptake [9]. SLN obtained by coacervation exceed the 200 nm limit, but being stabilized by non ionic surfactant-polymers, and considering the interesting results from preliminary *in vitro* studies, [8], the study of their *in vivo* fate is worthy of interest.

The association between the conjugate and the lipid matrix can cause that the *in vivo* pharmacokinetics and biodistribution are driven by the lipid component. To this aim, in this experimental study, ddMTX-loaded SLN were preliminarily assayed *in vivo* in healthy rats for biodistribution. Functionalization with a chimera peptide, having a lipophilic moiety and an aminoacidic sequence for VLDL receptor binding (ApoE), was exploited in order to target SLN to VLDL receptor, owing to a similar procedure employed for LDL receptor targeting [10]. The potential of VLDL receptor on endothelial cells for BBB targeting is an established concept in literature [11]. The potentiality of this approach for GBM treatment was preliminarily studied in a previously developed syngeneic F98/Fischer rat glioma model [11], through MRI and immunohistochemical analysis.

2. Materials

2.1 Chemicals and reagents

Sodium behenate (SB) was from Nu-Chek Prep, Inc. (Elysian, U.S.A.); DMSO, methotrexate (MTX), and 80% hydrolyzed polyvinyl alcohol 9000–10000 Mw (PVA 9000) from Sigma (Dorset, UK); sodium dodecyl sulfate (SDS) was from Fluka (Buchs, Switzerland); TRIS, phosphoric acid, hydrochloric acid, sodium hydroxide and sodium phosphate monobasic from Merck (Darmstadt, Germany); Br-dodecane, dichlorometane, chloroform, methanol and ethanol from Carlo Erba (Val De Reuil, France); ApoE chimera peptide was from Genscript (Piscataway, NJ, USA): amino acid sequence DWLKAFYDKVAEKLKEAFLRKLKRLLLRKLKRL; acetylation on N-Terminal and C-terminal; the 36 amino acid sequence consists of 18-amino acid amphipathic alpha helix and 18 VLDL receptor binding domain (in *italics*); MW 4560 Da; deionized water was obtained by a MilliQ system (Millipore, Bedford, MO). All other chemicals were analytical grade and used without any further purification.

Electrophoresis reagents were from Bio-Rad Laboratories (Hercules, CA). The protein content of cell lysates was assessed with the BCA kit from Sigma Chemicals Co (St. Louis, MO). When not otherwise specified, all the other reagents were from Sigma Chemicals Co.

2.2 Cells

Rat F98 glioma cells were obtained from LGC Standards S.r.l. (Sesto San Giovanni, MI Italy) and maintained in a humidified incubator gassed with 5% CO₂ (37 °C) with Dulbecco's Modified Eagle's Medium (DMEM) supplemented with 10% Fetal Bovine Serum (FBS) and 1% antibiotic/antimycotic solutions. The day of the surgery, cells were trypsinized, centrifuged, counted and re-suspended at 100.000 cells/2µl in DMEM + agar 1%.

2.3 Animals

Wistar and Fischer male rats (Charles River, Wilmington, MA) 200-250 g weighting, were housed in standard facilities, handled and maintained according to our Institutional Animal Care and Use Committee ethical regulations. Rats were kept under controlled environmental conditions (23 ± 1 °C, 50–60% humidity, 12 h light and dark cycles, lights on at 7:00 a.m.). Rats were given *ad libitum* access to food and water. The procedures conformed to the Ethics Committee of University of Turin's institutional guidelines on animal welfare (DL 116/92) as well as International Guidelines and all efforts were done to minimize the number of animals and their discomfort. All experiments on animal models were performed according to an experimental protocol approved by the University Bioethical Committee and the Italian Ministry of Health (prot. n. 0135/2015).

2.4 ddMTX synthesis

ddMTX was synthesized according to literature [13, 14].

2.5 SLN preparation

2% behenic acid (BA) 4% PVA 9000 SLN were prepared according to the coacervation method [3]. Briefly, SB was dispersed in water with PVA 9000 and the mixture was then heated under stirring (300 rpm), to obtain a clear solution (80 °C). 2 mg ddMTX were dissolved in 300 µl ethanol at 65 °C, prior to be added to 2.5 ml 2% SB 4% PVA 9000 micellar solution. The acidifying solutions (coacervating solutions – 0,4 ml 1M sodium di-hydrogen phosphate and 0,6 ml 1M hydrochloric acid) were added drop-wise to the mixture until complete BA precipitation occurred. The obtained suspension was then cooled under stirring at 300 rpm until 15 °C temperature was reached [8] (Figure 1). The suspensions were then concentrated under nitrogen steam to a 2.5 ml final volume.

2.6 SLN functionalization with ApoE

2.5 ml SLN were incubated at room temperature for 1 hour with a concentrated aqueous solution of ApoE to give a 0.1 mg/ml final concentration in SLN suspension, the purification from unbound protein was then performed as follows: *a*) by gel filtration, using a matrix of cross-linked agarose (Sepharose CL 4B – size exclusion 100000 Da) as stationary phase; *b*) by gel centrifugation, using cross-linked polyacrylamide (Biogel P-6 – size exclusion 6000 Da); *c*) by dialysis (14000 Da membrane cut-off). Since sample dilution occurs after gel filtration, the opalescent fractions containing the purified SLN were concentrated under nitrogen steam up to 1 ml final volume (Figure 1).

Chimera peptide binds to SLN surface by simple electrostatic interaction. The effective functionalization was assessed by SDS gel electrophoresis (12% polyacrylamide) performed in non denaturing conditions, followed by staining with 10 ml Coomassie Blue solution (0.2% w/v Coomassie Blue, 7.5% v/v acetic acid, 50 % v/v ethanol), for 1 hour at room temperature, and by overnight de-staining with deionized water. The amount of ApoE associated to SLN was quantified at the same time with the BCA kit.

2.7 SLN characterization

SLN particle sizes and polydispersity indexes (PDI) were determined 1 hour after preparation using dynamic light scattering technique-DLS (Brookhaven, New York, USA). Size measurements were obtained at an angle of 90° at 25 °C. All data were determined in triplicate.

ddMTX concentration was determined in suspension just after preparation and after SLN purification from untrapped drug, obtained as previously described for ApoE.

ddMTX entrapment efficiency (EE%) of SLN was determined as follows: 0.5 ml SLN suspension was diluted with 0.5 ml water and centrifuged for 15 min at 62000 g (Allegra 64R centrifuge, Beckmann Coulter, Brea, CA, USA); the precipitate was washed with 1 ml 30:70 v/v ethanol:water to eliminate adsorbed drug. The lipophilic prodrug was extracted from the solid residue in 1 ml

dichloromethane and injected into silica-HPLC (PDA detector at 302 nm). Basing on EE% the drug loading (mg drug/mg lipid) was calculated.

Moreover, the final prodrug content in SLN suspension was also determined with fluorescence RP-HPLC after 500-fold water dilution and derivatization.

2.8 HPLC analysis

Analyses were performed with a YL9100 HPLC system equipped with a YL9110 quaternary pump, a YL 9101 vacuum degasser and a YL 9160 PDA detector and/or a Shimadzu RF-10A fluorescence detector (Shimadzu, Tokyo, Japan), linked to YL-Clarity software for data analysis (Young Lin, Hogyedong, Anyang, Korea).

RP-HPLC method was developed for the determination of both MTX and ddMTX in biological samples, starting from a literature method [15]. Briefly, 0.25 ml samples were added of 0.1 ml 10% SDS aqueous solution, in order to promote ddMTX dissolution; then they were de-proteinized with 0.08 ml 10% TCA and centrifuged. 0.2 ml of the supernatant were added of 0.05 ml 5M pH 5.0 acetate buffer. MTX or ddMTX were then oxidized to fluorescent pteridin carboxylic acid with 0.05 ml 5% KMnO₄. HPLC analysis was performed with Teknokroma Mediterranea Sea RP 2.5 μm 125×4.6mm column. 0.05 M pH 6.7 TRIS buffer (adjusted with phosphoric acid) was used as mobile phase at 1 ml min⁻¹ flow. After peak elution, gradient was performed with 30% acetonitrile in order to clean the column from reaction sub-products. Retention time was 12 min.

For ddMTX analysis Teknokroma Kromosil 100TM, 250×4.6 mm, 2.5 μm particle size was employed. HPLC grade dichloromethane/methanol (95/5 v/v) was used as a mobile phase with a flow rate of 1 ml min⁻¹. PDA detector was set at 302 nm. Retention time was 10 min [8].

2.9 *In vitro* cytotoxicity against F98 cells

The cytotoxic effect of free MTX and ddMTX-loaded SLN against F98 tumor cells was evaluated *in vitro*, assessing cell viability by the Trypan blue dye exclusion test. Briefly, cells were plated at a

density of 200×10^3 cells in 5 ml medium in a 25 cm² flask, allowed to grow for 24 hours and then treated with 0.5 and 5 μ M MTX (free in solution, or as ddMTX entrapped in SLN) for 72 hours at 37° C in a 5% O₂/CO₂ atmosphere. ddMTX was not used as control, because of its very low solubility in medium. The number of viable cells was determined using a TC20 automated cell counter (Bio-Rad) and cytotoxicity was expressed as number of surviving cells as percentage of control (untreated cells). Cell viability was also measured after treatment with 5 and 50 μ M TMZ, as positive control, and, in order to verify the non-toxicity of the carriers, with unloaded SLN at the concentration corresponding to that used for entrapped drugs. All experiments were performed in quadruplicate.

2.10 Analysis of apoptosis in F98 cells

The active Caspase-3 protein expression was determined using immunocytochemistry. After 48 h exposure to 5 and 50 μ M TMZ, 0.5 and 5 μ M free or SLN-entrapped ddMTX and to empty SLN, cells were fixed for 30 min with 4% paraformaldehyde at room temperature and then the immunostaining reaction was performed using a Ventana Full BenchMark® XT automated immunostainer (Ventana Medical Systems Inc., Tucson, AZ, USA) with UltraView™ Universal DAB Detection kit (Ventana Medical Systems Inc.) as detection system. Primary antibody was rabbit anti-cleaved Caspase 3 (Asp175), dilution 1:300. Observations were done on a Zeiss Axioskop fluorescence microscope (Carl Zeiss, Oberkochen, Germany) equipped with an AxioCam5 MR5c and coupled to an Imaging system (AxioVision Release 4.5; Carl Zeiss).

Following the same treatments as for cleaved Caspase 3 analysis, *in situ* terminal deoxynucleotidyl transferase-mediated dUTP-biotin nick end-labeling (TUNEL) assay was performed using the *in situ* cell death detection kit, fluorescein (Roche, Diagnostic Corp., Indianapolis, IN, USA) according to the manufacturer's instructions.

Apoptotic indexes were calculated as the mean number of cleaved Caspase-3-positive cells or TUNEL-positive cells counted in five randomly selected microscopic fields at 400x

magnification; the number of apoptotic cells was expressed as percentages of the total cell number, which, however, represented a quota in comparison with untreated cells.

2.11 Biodistribution studies

ddMTX loaded SLN, with or without ApoE (1,6 mg/kg ddMTX corresponding to 1 mg/kg MTX) and di-sodium MTX (1 mg/kg) solution in normal saline were administered through a catheter surgically positioned in the jugular vein of male Wistar healthy rats (weight 250 g). ddMTX was not used as control, because of its very low solubility in water, that hampers its i.v. administration as free molecule. At scheduled times (30 minutes and 90 minutes after administration) rats were sacrificed by CO₂-induced euthanasia, plasma was withdrawn and organs (liver, spleen, kidneys, lungs, heart, brain) were removed surgically. Each experiment was performed on four rats for each sample administered.

A pilot biodistribution experiment was also performed by using 7 days implanted glioma models, described below, aiming to detect differences between biodistribution in healthy rats and glioma models. Glioma model carrying rats were sacrificed 30 minutes after administration.

Organs were homogenized with UltraTurrax[®] (IKA, Staufen, Germany) for 5 min in water at a tissue concentration of 125 mg/ml; tissue homogenates and plasma underwent the derivatization reaction prior to fluorimetric HPLC detection [15].

2.12 Glioma model

Fischer rats were anesthetized by 1.5%–2.5% isoflurane and 0.8 l/min oxygen and then fixed in a stereotactic apparatus. 100.000 F98 glioma cells in 2µl DMEM+agar 1% were injected stereotactically in Fischer rats respectively. A 1.2 mm burr hole was drilled into the right side of the skull (2.5 mm anterior and 2 mm lateral to the bregma) to expose the *dura mater*. Using a microliter syringe equipped with a 26-gauge needle and connected to the manipulating arm of the stereotactic apparatus, glioma cells were injected into the caudate nucleus at a depth of 6 mm from the *dura*

mater over a 5 min period. A trypan blue exclusion test was performed to assess cell viability before implantation and cells viability was always > 95% [11].

After surgery, animals were treated with Ketoprofen (10 mg/ml): 2.5 mg/kg once a day at 48 h intervals first and second weeks; 5 mg/kg once a day at 48 h intervals third week; 5 mg/kg/ once a day and were housed routinely. At the end of the experiment (11 days after tumour cells implantation), animals were anesthetized with Zoletil 100 0.1 ml/kg i.p. and euthanized with CO₂.

2.13 Experimental protocol

Efficacy of ddMTX-loaded SLN ApoE towards syngeneic F98/Fischer glioma model was assayed following administration of SLN at a 1.6 mg/kg ddMTX dose (corresponding to 1 mg/kg MTX) at day 7 and 9 after implantation (6 animals), according to a modified literature method [16]. IV administration was performed by injection in the tail vein. Untreated rats were used as controls (8 animals), while positive controls were obtained by administering oral TMZ (current pharmacological adjuvant treatment for GBM) at days 7, 8, 9, 10 with a dose of 7 mg/kg (4 animals).

2.14 MRI

Glioma growth was monitored at different times (day 7, 9, 11 after implantation), through magnetic resonance imaging (MRI), using a high-field (7T) horizontal bore magnet (Bruker Pharmascan MRI, Germany). Rats were anesthetized with 2% isoflurane in an oxygen/air mixture (1:1) at a flow rate of 3 l/min and placed in a MR probe in a supine position. The respiration rate (typical range, 30-50 breaths/min) of the animals was monitored throughout the whole experiment, using an abdominal pneumatic pillow. T₁-weighted images (15 transverse slices with a thickness of 1.5 mm and taken in a field of view (FOV) of 5.0x5.0 cm² with a matrix of 128x128 pixel) were acquired using a MSME (multislice spin-echos) sequence (TR/TE: 400/8.4 ms, number of averages: 6) on axial and coronal planes after i.v. injection of 0.5 mmol/kg of gadobenate dimeglumine

(MultiHance[®], Bracco Imaging, Milan, Italy) in the tail vein [11]. Glioma volume was evaluated through Bruker Pharmascan software: the brain was divided in 15 transverse slices of 1.5 mm thickness of, and the area evidenced by gadobenate dimeglumine (tumour) was approximated by the software. Final integration was performed between calculated areas and slice thickness.

2.15 Histology and immunohistochemistry on brain specimen

After euthanasia, all animals were submitted to a complete necropsy. Lung, heart, liver, kidney, spleen and brain were collected and stored in 10% neutral buffered formalin for histological evaluation. Slide sections (5 mm thick) were obtained using a microtome (Leica Microsystems, Wetzlar, Germany) and stained with hematoxylin and eosin stain. During brain evaluation, histological features were classified as positive if a tumor mass was present and negative if no tumor was detected.

Immunohistochemical staining was also done on selected sections. Primary antibodies included: two polyclonal, antibodies Cleaved Caspase-3 (Asp175) (1:300, Cell Signaling) and glial-fibrillary acidic-protein (GFAP; rabbit anti-cow GFAP; 1:2,000 dilution; code number Z0334; Dako), and one monoclonal antibody Ki-67 (1:100 dilution; code M7248; Dako, Carpinteria, CA).

Antibodies were detected using the avidin–biotin–peroxidase complex technique with the Vectastain ABC-AP Kit (Universal) (Vector Laboratoires, Burlingame, Ca, USA).

Antigen retrieval was done by heating the sections in citrate buffer (0.01 M, pH 6.0) at 98 °C for 25 min. Endogenous peroxidase activity was quenched by incubating the specimen for 5 min in 3% hydrogen peroxide at room temperature. The slides were then incubated overnight in a humidified chamber at 4 °C with the primary antibodies, followed by sequential 10-min incubations with biotinylated link antibody and peroxidase-labeled streptavidin. The reaction was visualized using 3,3'-diaminobenzidine tetrahydrochloride (DAB, Sigma-Aldrich, St. Louis, MO, USA). The nuclei were counterstained with hematoxylin and eosin stain. Positive and negative immunohistochemistry controls were routinely used.

In situ terminal deoxynucleotidyl transferase-mediated dUTP-biotin nick end-labeling (TUNEL) assay was performed by means of the *in situ* cell death detection kit, fluorescein (Roche, Diagnostic Corp., Indianapolis, IN, USA) according to the manufacturer's instructions.

The reproducibility of the staining was confirmed by re-immunostaining via the same method in multiple, randomly selected specimens.

All reactions were visualized by light microscopy using an Olympus Provis AX70 microscope equipped with a digital camera. Quantification of the staining was done by using an Image Pro Plus analysis system. Each immunohistochemical marker was evaluated in at least 10 different fields, and particularly measuring the numbers of positive cells for cleaved caspase-3 and Ki-67.

2.16 Statistical Analysis

GraphPad Prism® software was used to perform statistical analysis. Shapiro–Wilk's test was used to establish normality or non-normality of distribution. The one-way Kruskal–Wallis test and Dunn post hoc test were performed to investigate differences among the groups when the data did not follow the normal distribution. Student test was employed to calculate P values for data following normal distribution. P values < 0.1 were considered statistically significant. Data were expressed as median and standard deviation.

3. Results and discussion

ddMTX loaded SLN were prepared according to Annovazzi et al. [8]: basing on Annovazzi and co-workers' *in vitro* studies, good drug entrapment efficiency was demonstrated, as well as cytotoxic activity against primary human GBM cultures. Moreover, promising uptake by endothelial cells was demonstrated in artificial BBB models.

In this experimental work, such formulation was tested *in vivo* in animal models. Indeed, despite the encouraging results obtained with artificial BBB models and plain ddMTX-loaded SLN, appropriate *in vivo* studies are required to support preliminary *in vitro* results. It is well recognized that animal

models are more complex than *in vitro* systems, and biodistribution and clearance by RES organs of systemically administered drug delivery systems can actually influence the drug amount presenting to the BBB.

To this aim, ApoE was used, a chimera peptide able to bind the VLDL receptor and to anchor to the lipid surfaces, as already demonstrated with liposomes [10]. In the formulation development, particular care was given to evaluate and to select a suitable purification technique, based on molecular size exclusion, for ddMTX-loaded SLN ApoE. The optimization of the technique was not only aimed to purification purposes, but also to check both the entrapment efficiency of ddMTX and the binding of ApoE to SLN. Different molecular size cut-off were used in gel centrifugation (6000 Da) and gel filtration (100000 Da) techniques.

SLN functionalized with ApoE were resolved by SDS-PAGE followed by Blue Coomassie staining. As shown in Figure 2, the amount of ApoE bound to SLN was identified, since it didn't run in the gel, due to high size of nanoparticles, compared to the free protein. Most ApoE circulates as dimer in plasma and cerebral spinal fluid, due to a disulphide bond between each monomer [17, 18]. We detected indeed both ApoE monomer and dimers in our standard. Only monomers were detected in SLN formulations. Purification with dialysis led to a greater ApoE leakage from nanoparticles compared to gel centrifugation and gel filtration. The spectrophotometric quantification of ApoE associated with SLN, performed by the BCA method, confirmed this trend (Table 1): basing on experimental data and considering the spherical shape of SLN with density corresponding to that of BA (0.82 g/ml), the ratio between ApoE and SLN was approximated. Moreover, unfunctionalized SLN showed a Zeta potential near to zero, because of PVA steric hindrance; ApoE functionalized SLN showed a slightly more negative Zeta potential (near -7 mV), also maintained after purification (table 1).

Both gel centrifugation and gel filtration removed a part of the ddMTX amount used to formulate drug loaded SLN, which was probably not entrapped in the lipid matrix; on the other hand, drug

leakage was larger after dialysis, probably because the extended times associated with dialysis bag method can cause partial release of entrapped drug, too.

Basing on these data, gel filtration was chosen as purification method for ddMTX loaded SLN ApoE in the subsequent experiments. Preliminarily to following experiments, stability of ddMTX loaded SLN, both unfunctionalized and ApoE functionalized, was confirmed after dilution with normal saline (Table 1).

Prior to *in vivo* testing of the formulations, their toxicity against glioma cells used in the *in vivo* glioma model was assessed. In the presence of both free and SLN-entrapped ddMTX, the *in vitro* proliferation of F98 rat tumor cells was inhibited, as already observed for human GBM cell lines [8]. After 72-h exposure, cells were rounded in appearance, unable to adhere and, compared with untreated cells, a significant reduction of cell viability was observed with 0.5 μ M and even more with 5 μ M drug. At this latter concentration, the number of surviving cell was almost negligible, indicating a growth inhibitory effect even higher of that induced by TMZ, the standard of care in chemotherapy of GBM patients (Figure 3).

Experiments demonstrated that the cytotoxicity of SLN-loaded ddMTX at the two concentrations analyzed was maintained or was slightly lower than the free drug solution. The exposure of the cells to unloaded SLN at the highest SLN concentration used for the study determined only a mild reduction of cell viability, suggesting the safety of SLN under study (Figure 3).

In order to establish whether the antiproliferative activity of the drug had cytostatic effects or was followed by cytotoxic consequences, we investigated cell death occurrence in both control and drug treated tumor cells. We employed two common methods to determine apoptosis: the immunocytochemical determination of the activated Caspase 3 and the TUNEL assay.

We observed an enhanced expression of cleaved Caspase 3 after treating the cells with free MTX or SLN-entrapped ddMTX and the level of expression was almost the same for free and for SLN-entrapped drug, increasing in a dose-dependent manner; moreover, at 5 μ M concentration, the percentage of apoptotic cells obtained with both free and SLN-entrapped MTX was quite higher

than that with TMZ at the same concentration. With the TUNEL assay, a lower rate of apoptosis was detectable, but the general trend was confirmed.

The discrepancy observed between the results obtained with the two assays can be explained taking into account that activation of Caspase 3 is a relatively early event in the apoptotic process and allows detection of cells in the initial stages of apoptosis, whereas the DNA fragmentation, revealed by TUNEL method, is a late event and could be a characteristic not only of apoptotic but also of necrotic cells.

It is noteworthy that after 48 h treatment with TMZ the effect on cell death was better evidenced with TUNEL assay, whereas activation of Caspase 3 was more visible after treatment with free and SLN-loaded MTX. This difference is likely due to the different action mechanisms of the two drugs. Probably, TMZ at 50 μ M concentration could induce a precocious cell death in F98 cells and, already after 48 h, most cells displayed DNA fragmentation detectable with TUNEL. This method can evidence not only the apoptotic process, but also other types of cell death and, in fact, according to some authors [19], TMZ cytotoxicity on malignant glioma cells can result in an autophagic rather than apoptotic cell death.

On the contrary, the activation of Caspase 3, specific marker of the early stages of apoptotic process, resulted higher in MTX-treated cells, compared to untreated cells, indicating that the drug is able to induce cell death through apoptosis.

Occurrence of apoptosis after treatment with unloaded SLN was similar to that showed by untreated cells.

The percentages of apoptotic cells measured with both methods following the treatments is shown in Figure 4.

These results clearly indicated that the toxicity on F98 rat glioma cells, mediated by the induction of apoptotic death of ddMTX-loaded SLN is due to entrapped ddMTX and not to the nanosystem, as unloaded SLN revealed to be safe against the same cells. As far as we know, ddMTX has not yet studied as *in vitro* PGP substrate. Our hypothesis, based on literature [2], is that SLN might enter

the cells by an endocytosis mechanism, bypassing the PGP system, regardless of the fact that ddMTX is a substrate of the PGP.

In *in vivo* biodistribution experiments on healthy rats showed drug accumulation in RES organs, following SLN administration; however, a significantly lower drug removal from plasma and organs was observed after ddMTX-loaded SLN administration compared to the parental drug (MTX) solution (Figure 5A and 6A). ApoE was important to increase drug amount recovered in the brain, also if it's difficult to evaluate, from these preliminary data, whether an active targeting can be present., and its effect was evident especially at longer times after administration, compared to non functionalized SLN and free drug (Figure 6B). Since it is well known from literature [20] that the altered BBB in the glioma can increase the uptake of molecules and small nanoparticles, similar biodistribution experiments were performed in rat glioma models: no difference was noted compared to healthy rats, probably because SLN size exceeds the small fenestrations of altered BBB.

The obtained *in vivo* biodistribution of nanoparticles is influenced by different factors: one of the most important should be particle size, whereas nanoparticles smaller than 200 nm are considered to be able to exclude splenic filtration, and, if coated by hydrophilic polymers, to avoid opsonization. Particles with size in the 200-500 nm range can avoid splenic filtration, owing to surface characteristics and deformability [21, 22]. Long circulation of nanoparticles should be a key point for brain delivery, allowing a prolonged contact with endothelial cells.

In this experimental work, 350 nm SLN have been engineered, but no specific pharmacokinetic study was planned. However, from plasmatic concentrations obtained at 0.5 and 3 hours in biodistribution experiments, it can be observed that ddMTX loaded SLN show increased plasmatic residence compared to free MTX: this can be probably ascribed to SLN and can contribute to brain accumulation.

Moreover, the capability of PBCA nanoparticles larger than 200 nm to successfully overcome BBB is documented by a recent publication [9]: interestingly, t nanoparticles surface chemistry, and not

particle size, resulted to be the parameter with the most significant influence on BBB passage. It was hypothesized that some non-ionic surfactants allow adsorption of ApoE from the blood and BBB passage via the specific transporter system. SLN by coacervation described in the present work are stabilized by non ionic polymers with surface activity; the addition of exogenous ApoE through a chimera peptide can promote brain accumulation.

To this regard, it should be considered that the receptor binding sequence in the chimera peptide is that corresponding to ApoE2, which is the main ligand for VLDL receptor: VLDL receptors are abundantly expressed in heart, muscle adipose tissue and brain, and are barely expressed in the liver, where LDL receptors are expressed abundantly [23]: consequently, even if not selectively specific for the brain, the VLDL receptor could be a good compromise to enhance brain accumulation of SLN.

Nevertheless, the aim of this preliminary biodistribution study excludes the clear demonstration of a precise role of VLDL targeting in the increase of brain uptake: in fact, in order to demonstrate such hypothesis, further studies on rat brain should be performed, like brain perfusion or capillary depletion, after sacrifice of the animal [24]. These assays would allow to exclude or quantify, respectively, the accumulation of drug in brain capillaries, compared to brain parenchyma. Moreover competition assays should be performed, by administering ddMTX loaded SLN ApoE together with free ApoE, in order to selectively assess that ApoE binding to VLDL receptor is responsible for BBB overcoming. Anyway, the variables associated to *in vivo* biodistribution experiments (unwanted ApoE-mediated targeting to other organs, peptide-induced opsonization and macrophage uptake...) would make it hard to obtain final conclusion also from competition experiments. And only partial and controversial explanation could be obtained by loading/adsorbing on SLN a model protein to mimic biodistribution/opsonization process due to proteins, because of the different tissue selectivity of various proteins.

The main goal obtained from these preliminary biodistribution experiments is the enhancement of drug brain accumulation by SLN, confirming the promising *in vitro* experiments from previous

work [8]. *In vitro* BBB models previously employed [8] are static systems, and the shift to *in vivo* biodistribution needs the improving of brain uptake with targeting strategies. To this aim, a partially selective brain receptor (receptor for VLDL) was chosen, and a simple functionalization strategy employed. In this way, conjugation reactions are avoided, and high molecular weight peptides, which are expensive and responsible for most of the opsonization processes are substituted with a short chimera peptide.

In order to hypothesize their potentiality for GBM treatment, preliminary efficacy experiments on the syngeneic F98/Fischer glioma model were then performed with ddMTX loaded SLN ApoE. No free MTX or unfunctionalized SLN were employed, because biodistribution data revealed negligible drug brain accumulation. The rapid onset and exponential growth of this glioma model makes it suitable to mimic some of the human GBM conditions. Oral TMZ was employed as positive control, since it is the standard of care in chemotherapy of GBM patients, according to literature protocols [25], but given the different administration routes (oral vs i.v.), dosing schedules and drug dosage (compared to SLN), no relation can be hypothesized between drug brain concentration and efficacy. Tumor volume, measured through MRI, increased very fast, starting from one week after implantation. Treatment with ddMTX-loaded SLN ApoE resulted in a mean decrease of tumor volume growth, compared to control and to oral TMZ: the calculated P value at day 11 after implantation was slightly higher than 0.1 for control vs SLN, and higher than 0.1 for control vs TMZ, and consequently was not reported (Figure 7).

All GBM showed similar histopathological hallmarks, regardless they were belonging to treated or control rats. Tumors were composed of variably sized, irregular, rounded or elongated fusiform cells, nearly always arranged in a lobular pattern. Multifocal necrosis and mitotic figures were present in all the tumors. Parenchymal invasion was abundant and characterized by small to voluminous neoplastic cells abutting adjacent blood vessels and invading the adjacent brain parenchyma. Moderate vascular proliferation was present at the peripheral margin. A very limited

and inconstant mononuclear inflammatory reaction was observed around the blood vessels surrounding the tumor masses [11].

GFAP was strongly expressed by peripheral reactive glia, while a multifocal to diffuse expression of this marker was observed in the neoplastic cells, confirming their glial origin. Ki-67 staining revealed a high proportion of mitotic figures in all the tumors (Figure 8). Caspase 3 expression and TUNEL assay in the tumor masses was different on the basis of the treatment: rats treated with ddMTX loaded SLN ApoE showed increased apoptosis compared both to negative and positive controls (TMZ) (Figure 9). In Figure 10 apoptosis is evaluated according to Caspase-3 quantification in glioma specimen: median values are lower for rats treated with ddMTX loaded SLN ApoE, but differences compared to controls were not significant .

4. Conclusions

In a previous experimental work, ddMTX loaded SLN, prepared according to the coacervation method, were tested *in vitro* by our research group, for cytotoxicity against GBM human primary cultures, and for permeation through artificial BBB models. Encouraging results obtained drove us to perform a preliminary test of this formulation on a F98/Fischer glioma model, previously studied by our research group. Given the complexity of drug distribution *in vivo*, SLN conjugation with an ApoE mimicking chimera peptide was performed and checked with electrophoresis, in order to obtain a supplementary accumulation to the brain. Biodistribution studies in healthy rats assessed the superiority of ApoE conjugated formulation, which was employed in efficacy studies. No difference in brain uptake was revealed between healthy rats and glioma models, probably because particle size exceeds fenestrations of glioma altered BBB. Differences were observed in tumor growth rate (measured through MRI), as well as in apoptosis between control and treated rats, even if not significant. *In vitro* tests on F98 cultured cells assessed their susceptibility to treatment, with consequent apoptosis, and allowed us to hypothesize a direct correlation between the *in vitro* results on cells and the apoptosis observed *in vivo* after treatment..

Despite some encouraging results, the efficacy of the treatment cannot be considered sufficient: a poor concentration in the brain may be considered as the main limit. In perspective to future studies, reduction of particle size and polydispersity, to be obtained by a technological approach, should be exploited to address this critical point.

5. Acknowledgements

The authors thank Fondazione San Paolo (Development of solid lipid nanoparticles (SLN) as vehicles of antineoplastic drugs to improve the pharmacological glioblastoma therapy - ORTO11WNST) and Italian MIUR (Ricerca Locale 2014) for funding.

6. References

1 - Karim R., Palazzo C., Evrard B, Piel G. Nanocarriers for the treatment of glioblastoma multiforme: Current state-of-the-art. *J. Control. Release* 227, 23–37 (2016).

2 - Wong HL, Bendayan R., Rauth AM, Li Y, Wu XY. Chemotherapy with anticancer drugs encapsulated in solid lipid nanoparticles. *Adv. Drug Del. Rev.* 59, 491–504 (2007).

* of interest: it describes the rationale for SLN in cancer treatment

3 - Battaglia L, Gallarate M, Cavalli R., and Trotta M. Solid lipid nanoparticles produced through a coacervation method. *J. Microencapsul.* 27 (1), 78–85 (2010).

** of considerable interest: it concerns an innovative technique for SLN preparation

4 - Battaglia L, Serpe L, Muntoni E, Zara GP, Trotta M, Gallarate M. Methotrexate loaded SLNs prepared by coacervation technique: in vitro cytotoxicity and in vivo pharmacokinetics and biodistribution. *Nanomedicine (London)* 6, 1561-1573 (2011).

* of interest: it concerns an methotrexate entrapment in SLN

5 - Battaglia L, Gallarate M, Peira E, et al. SLN for potential doxorubicin delivery in glioblastoma treatment: preliminary in vitro studies. *J. Pharm. Sci.* 103, 2157-65 (2014).

6 - Gallarate M, Trotta M, Battaglia L, Chirio D. Cisplatin loaded SLN produced by coacervation technique. *J. Drug Del. Sci. Technol.* 20, 343-347 (2010).

7 - Chirio D, Gallarate M, Peira E, et al. Positive-charged solid lipid nanoparticles as paclitaxel drug delivery system in glioblastoma treatment. *Eur. J. Pharm. Biopharm.* 88, 746–758 (2014).

8 - Annovazzi L, Schiffer D, Mellai M, et al. Solid lipid nanoparticles loaded with antitumor lipophilic prodrugs aimed to glioblastoma treatment: preliminary studies on cultured cells. *J. Nanosci. Nanotechnol.* in press

** of considerable interest: it concerns a prodrug approach to load hydrophilic anticancer drugs in SLN

9 - Voigt N, Henrich-Noack P, Kockentiedt S, Hintz W, Tomas J, Sabel BA. Surfactants, not size or zeta-potential influence blood–brain barrier passage of polymeric nanoparticles. *Eur J Pharm Biopharm* 87, 19–29 (2014)

10 - Nikanjam M, Gibbs AR, Hunt CA, Budinger TF, Forte TM. Synthetic nano-LDL with paclitaxel oleate as a targeted drug delivery vehicle for glioblastoma multiforme. *J. Control. Release* 124, 163–171 (2007).

** of considerable interest: it concerns a simple way to obtain brain targeting

11 - Wyne KL, Pathak RK, Seabra MC, Hobbs HH. Expression of the VLDL Receptor in Endothelial Cells. *Arterioscler Thromb Vasc* 16, 407-415 (1996)

12 - Biasibetti E, Valazza A, Capucchio MT, et al. Comparison of an allogeneic and a syngeneic rat glioma model through MRI and histopathological investigations. *Comparative Med*, in press

* of interest: it describes variability among rat glioma models used to assess efficacy of pharmacological treatment

13 - Rosowsky A, Forsch RA, Yu CS, Lazarus H, Beardsley GP. Methotrexate Analogues. 21. Divergent influence of alkyl chain length on the dihydrofolate reductase affinity and cytotoxicity of methotrexate monoesters. *J. Med. Chem.* 27, 605-609 (1984).

14 - Moura JA, Valduga CJ, Tavares ER, Kretzer IF, Durvanei A, Maranhão MRC. Novel formulation of a methotrexate derivative with a lipid nanoemulsion. *Int. J. Nanomed.* 6, 2285–2295 (2011).

15 - Nelson JA, Harris BA, Decker WJ, Farquhar D. Analysis of Methotrexate in Human Plasma by High-pressure Liquid Chromatography with Fluorescence Detection. *Cancer Res.* 37, 3970-3973 (1977).

16 - Jain A, Garg NK, Tyagi RK, et al. Surface engineered polymeric nanocarriers mediate the delivery of transferrin–methotrexate conjugates for an improved understanding of brain cancer. *Acta Biomater.* 24, 140–151 (2015).

17 - Weisgraber KH, Shinto LH. Identification of the disulfide-linked homodimer of apolipoprotein E3 in plasma. Impact on receptor binding activity. *J. Biol. Chem.* 266, 12029-12034 (1991).

- 18 - Montine KS, Bassett CN, Ou JJ, Markesbery WR, Swift LL, Montine TJ. Apolipoprotein E allelic influence on human cerebrospinal fluid apolipoproteins. *J. Lipid. Res.* 39, 2443-2451 (1998).
- 19 - Kanzawa T, Germano IM, Komata T, Ito H, Kondo Y, Kondo S. Role of autophagy in temozolomide-induced cytotoxicity for malignant glioma cells. *Cell Death Differ.* 11, 448-457 (2004).
- 20 - Yu Liu and Weiyue Lu. Recent advances in brain tumor-targeted nano-drug delivery systems, *Exp. Opin. Drug Deliv.* 9, 671-683 (2012).
- 21 - Moghimi SM, Porter CJH, Muir IS, Illum L, Davis SS. Non phagocytic uptake of intravenously injected microspheres in rat spleen: influence of particle size and hydrophilic coating. *Biochem Biophys Res Commun.* 177 (2), 861-866 (1991)
- 22 - Moghimi SM, Hunter AC, Murray JC. Long-Circulating and Target-Specific Nanoparticles: Theory to Practice. *Pharmacol Rev.* 53, 283–318 (2001)
- 23 - Takahashi S, Sakai J, Fujino T, et al. The very low-density lipoprotein (VLDL) receptor: characterization and functions as a peripheral lipoprotein receptor. *J Atheroscler Thromb.* 11(4): 200-208 (2014)
- 24 - Triguero D, Buciak J and Pardridge WM. Capillary depletion method for quantification of blood-brain barrier transport of circulating peptides and plasma proteins. *J Neurochem.* 54(6): 1882-1888 (1990)

25 - Dagıstan Y, Karaca I, Bozkurt ER, et al. Combination hyperbaric oxygen and temozolomide therapy in c6 rat glioma model. *Acta Cirúrgica Brasileira* 27(6), 383-387 (2012)

Figure captions

Figure 1: Schematic representation of SLN formulation and functionalization

Figure 2: Representative photographs of the SLN ApoE after electrophoresis resolution and Coomassie Blue staining.

Figure 3: cytotoxicity against F98 cells at 72 hours; * $p < 0.01$ between control and TMZ (5 and 50 microM), control and MTX (0,5 and 5 microM), control and ddMTX loaded SLN (0,5 and 5 microM)

Figure 4: apoptosis of F98 cells; * $p < 0.01$ between control and TMZ 50 microM (TUNEL assay); between control and MTX 5 microM and between control and ddMTX loaded SLN 5 microM (Caspase 3) ** $p < 0.05$ between control and MTX 5 microM and between control and ddMTX loaded SLN 5 microM (TUNEL assay); between control and TMZ 50 microM (Caspase 3)

Figure 5: biodistribution of MTX and ddMTX loaded SLN 30 minutes after administration: A) organs; * $p < 0.1$: plasma ddMTX loaded SLN vs MTX and ddMTX loaded SLN glioma model vs MTX; ** $p < 0.05$ plasma ddMTX loaded SLN ApoE vs MTX B) brain; * $p < 0.1$: ddMTX loaded SLN ApoE vs MTX in brain

Figure 6: biodistribution of MTX and ddMTX loaded SLN 90 minutes after administration: A) organs; B) brain; * $p < 0,1$: ddMTX loaded SLN ApoE vs MTX and vs ddMTX SLN in brain

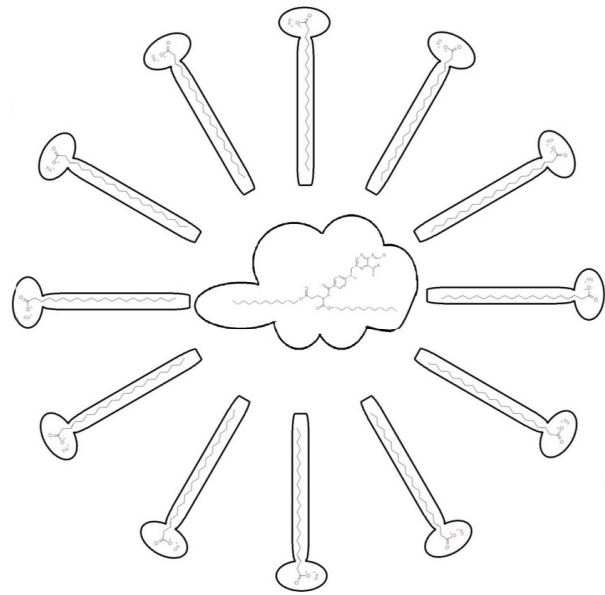
Figure 7: glioma growth curve (normalised to day 7)

Figure 8: Immunohistochemical staining of Ki67 in tumor sections. A control group, B ddMTX loaded SLN and C MTX, 40x.

Figure 9: Immunohistochemical staining of Caspase 3 in tumor sections. A control group, B ddMTX loaded SLN and C MTX, 40x.

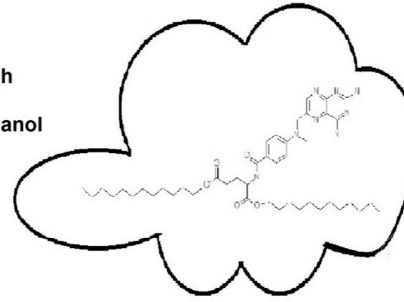
Figure 10: quantification of Caspase 3 expression in glioma specimen

| | Diameter (nm) | Polydispersity | Zeta Potential (mV) | ddMTX (mg/ml) | EE% | Drug loading (mg drug/mg lipid) | % ApoE (BCA assay) | Number ApoE for SLN | Diameter (nm) in normal saline | Polydispersity in normal saline |
|---|---------------|----------------|---------------------|---------------|-----|---------------------------------|--------------------|---------------------|--------------------------------|---------------------------------|
| ddMTX-loaded SLN | 322,9±7,8 | 0,270 | -2,44±0,86 | 0,691 | 86% | 0,014 | - | - | 327±5,0 | 0,24 |
| ddMTX-loaded SLN ApoE | 338,0±10,0 | 0,287 | -7,18±1,92 | 0,716 | 89% | 0,014 | 100% | 10942 | - | - |
| ddMTX-loaded SLN ApoE (gel filtrated) | 363,6±2,8 | 0,288 | -7,64±1,50 | 0,550 | 69% | 0,011 | 65% | 8810 | 360±5,8 | 0,25 |
| ddMTX-loaded SLN ApoE (dialyzed) | 370,5±2,5 | 0,237 | -5,64±0,90 | 0,310 | 39% | 0,006 | 47% | 6746 | - | - |
| ddMTX-loaded SLN ApoE (gel centrifuged) | 296,6±10,4 | 0,314 | -6,64±1,30 | 0,570 | 71% | 0,011 | 66% | 4850 | - | - |



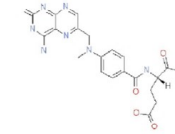
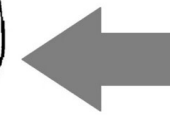
ddMTX loaded in sodium behenate micelles

micellization through pre-dissolution in a small amount of ethanol



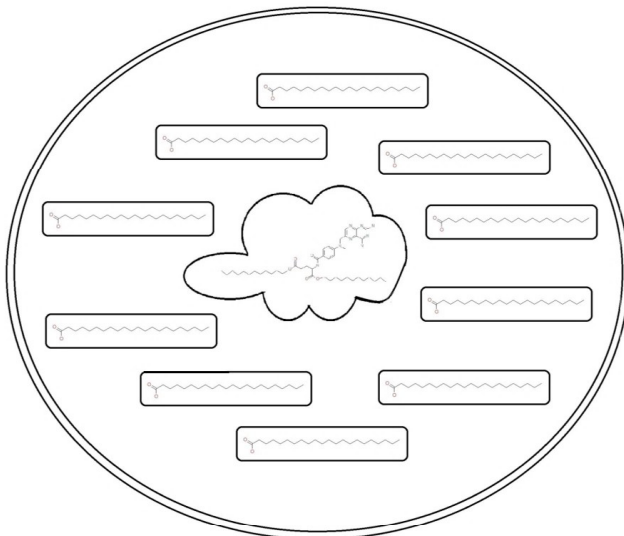
ddMTX

esterification



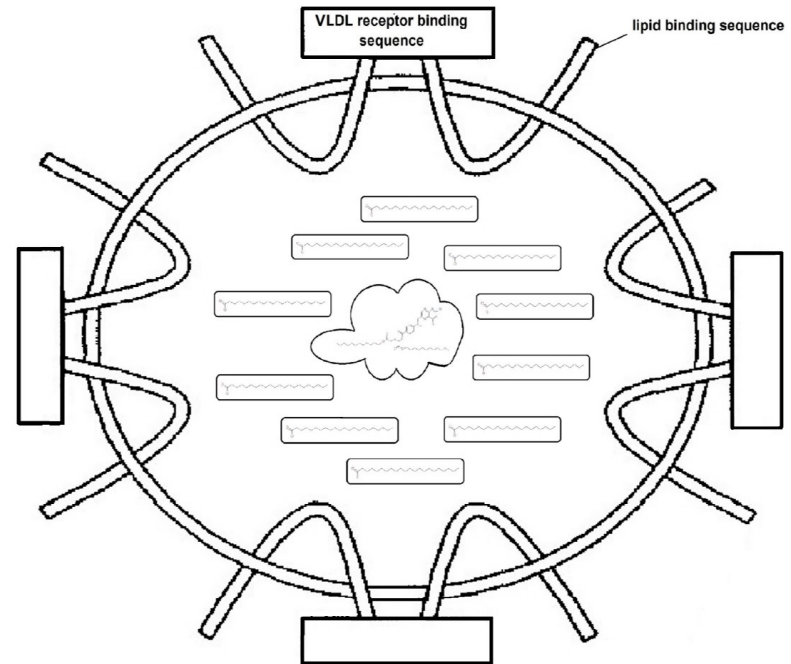
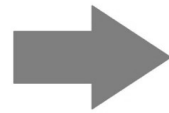
MTX

acidification

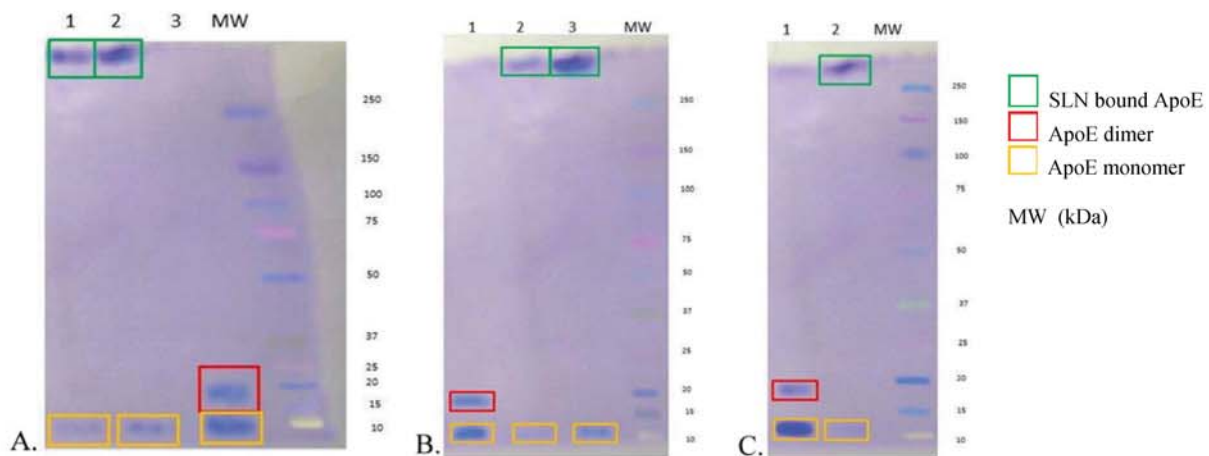


ddMTX loaded in behenic acid SLN through hydrophobic interactions between lipid and hydrophobic ddMTX chains

ApoE chimera peptide



ApoE chimera peptide coated behenic acid SLN containing ddMTX



A.
 1: ddMTX loaded SLN ApoE after gel filtration
 2: ddMTX loaded SLN ApoE before gel filtration
 3: ApoE

B.
 1: ApoE
 2: ddMTX loaded SLN ApoE after dialysis
 3: ddMTX loaded SLN ApoE before dialysis

C.
 1: ApoE
 2: ddMTX loaded SLN ApoE after gel centrifugation

